

## FAST FORWARD DETECTOR FOR MPD/NICA PROJECT: CONCEPT, SIMULATION, AND PROTOTYPING

*V. I. Yurevich*<sup>a,1</sup>, *O. I. Batenkov*<sup>b</sup>, *A. S. Veschnikov*<sup>b</sup>, *A. A. Povtoreyko*<sup>a</sup>,  
*S. P. Lobastov*<sup>a</sup>, *V. A. Babkin*<sup>a</sup>, *L. G. Efimov*<sup>a</sup>, *V. B. Dunin*<sup>a</sup>,  
*V. V. Tikhomirov*<sup>a</sup>, *D. N. Bogoslovsky*<sup>a</sup>, *G. S. Averichev*<sup>a</sup>, *G. A. Yarigin*<sup>a</sup>

<sup>a</sup> Joint Institute for Nuclear Research, Dubna

<sup>b</sup> Khlopin Radium Institute, St. Petersburg, Russia

Concept of a fast forward detector (FFD) developed as part of Multi-Purpose Detector (MPD) setup for future experiments with beams of nuclear collider NICA is described. The FFD is aimed at triggering nucleus–nucleus collisions at the center of the MPD setup and generating start pulse for TOF detector. Two units of the detector module were designed, produced, and tested with cosmic rays and proton beam. The time resolution obtained in the measurements is  $\sim 30$  ps (sigma). Results of simulation, prototype developing and experimental tests are discussed.

Представлена концепция быстрого переднего детектора FFD, создаваемого как часть многоцелевого детектора MPD для будущих экспериментов на пучках ядерного коллайдера NICA. Целью FFD является триггирование ядро-ядерных столкновений в центре установки MPD и генерирование стартового импульса для времяпролетного детектора. Разработаны, изготовлены и испытаны с космическими лучами и пучком протонов два детекторных модуля. Полученное в измерениях временное разрешение составляет  $\sim 30$  пс (сигма). Обсуждаются результаты моделирования, создания прототипа и экспериментальных испытаний.

PACS: 29.40.Ка; 29.40.Gx

### INTRODUCTION

Experimental study of a hot and dense nuclear matter formed in Au + Au collisions at the  $5 \leq \sqrt{s_{NN}} \leq 11$  GeV energy range has to be a major challenge for the ion collider NICA under development at JINR, Dubna [1]. To carry out such experiments, a Multi-Purpose Detector assembly (MPD) will be constructed and installed close to one of the two beams interaction points (IP) of the NICA [2]. The MPD consists of various detectors for studying characteristics of numerous secondary particles produced in IP within a wide interval of pseudorapidity. The fast forward detector (FFD) is one of them, and its aim is high-speed production of signals serving for the L0-trigger system with selection of nuclei collisions occurring close to IP and for generation of precise start pulse to activate the TOF detector.

---

<sup>1</sup>E-mail: yurevich@jinr.ru

Nowadays the R&D stage of the FFD project is realized and many questions regarding FFD functioning are under development and investigation. In this paper, we discuss the concept of FFD, MC simulation of the detector performance, a prototype of the FFD module and first experimental tests with proton beam and cosmic rays.

## 1. DETECTOR CONCEPT

High efficiency of the MPD operation implies detecting Au + Au collisions of any centrality with a time resolution  $\sigma_t \leq 50$  ps. We propose the FFD as a technical solution, according to this requirement.

An excellent time resolution should allow the FFD to function:

- (1) generating precise start signal for the TOF detector of the MPD;
- (2) producing pseudo-Vertex signal by fast identifying  $z$  position of collision along beam line with an accuracy of better than  $\pm 1.5$  cm;
- (3) initializing L0-trigger.

Besides, there are some additional important tasks where the FFD is a useful instrument. It can be of much help in adjustment of beam–beam collisions at the center of MPD setup and operative control of the collision rate and interaction point position during a run.

It is necessary to note that some similar fast detectors, of two arms to the left and to the right from IP, are already used with the same purpose in experiments at RHIC and LHC colliders.

In the PHENIX experiment, the Beam–Beam Counter (BBC) is used as the start detector [3]. It consists of two arrays of Cherenkov quartz counters located very close to the beam pipe at a distance of 144 cm from IP and covers the pseudorapidity range of  $3.0 < |\eta| < 3.9$ . A Hamamatsu R3432 fine mesh dynode PMT is used to detect the Cherenkov light. This PMT is capable of operating in strong magnetic fields. The fully implemented and installed BBC of 128 channels showed a single detector time resolution of  $(52 \pm 2)$  ps at RHIC for 130 GeV per nucleon Au + Au collisions [4].

The time-zero Cherenkov detectors [5] in the PHOBOS experiment are located at  $|Z| = 5.3$  m from IP. The resolution of each readout channel was about 60 ps after corrections on the slewing effect [6], which causes correlation between the time  $t$  recorded for a pulse and the size of the pulse, or amplitude  $A$ .

Two arrays of the ALICE T0 detector [7], each consisting of 12 PMTs, are located from IP at a distance of 70 cm on one side, covering the pseudorapidity range of  $2.9 < |\eta| < 3.3$ , and at 370 cm on an other side, covering the pseudorapidity range of  $5 < |\eta| < 4.5$ . The 3.0-cm-thick quartz Cherenkov radiators are optically coupled to the fine mesh dynode PMTs FEU-187, produced by Electron firm, Russia. In test runs with a beam of negative pions and kaons, the time resolution of 37 ps was obtained for the detector with 3.0-cm diameter radiator, and better time resolution of 28 ps was obtained with a smaller 2.0-cm diameter radiator [8].

The STAR start detector upVPD also consists of two identical arrays with 19 readout channels. Each readout channel consists of a Hamamatsu R5946 fine mesh dynode PMT, a Bicron BC420 scintillator, and a 6.4-mm Pb converter layer ( $\sim 1.13X_0$ ). The primary photons hit the Pb layer and generate by pair production process some ultrarelativistic electrons, which

come in the scintillator and produce scintillation light. The time resolution of single detector channel of 122 ps was measured in cosmic ray test [9].

At relatively low energies of NICA, the detectors have to match rather specific features of experimentation with the beams, which have velocities within the interval  $0.78 < \beta < 0.98$ , unlike experiments with the beams of ultrarelativistic energies at other colliders. In particular, the distinctive feature of a detector design for MPD/NICA is due to the fact that here secondary charged particles are mostly not relativistic within a large spread of velocities; moreover, the particle production is characterized by a much lower multiplicity. Therefore, an optimal solution in our case is to use a well-known phenomenon of multiple production of pions in central and semicentral collisions of heavy nuclei, where detection of the photons from neutral pions decays can help to reach the best timing.

Thus, the detector concept is based on the key idea, to register a fraction of high-rapidity photons along the beam line in both directions from IP. In the FFD, the high-energy photons are registered by their conversion to electrons inside a lead plate with thickness of  $\sim 1.5-2X_0$ . A similar method was realized in the STAR start detector. The electrons leave the lead plate and pass through a quartz radiator, generating the Cherenkov light with excellent time characteristics. Such a detector has high efficiency of registration for photons and charged particles with  $\beta > 0.69$ . The FFD consists of two subdetectors  $\text{FFD}_L$  and  $\text{FFD}_R$ , arranged as modular arrays and placed symmetrically along the beam line at a distance of 75 cm to the left and to the right from the MPD center (Fig. 1, *a*). Each subdetector array has a hole for the beam pipe and a pseudorapidity acceptance of  $2.3 < |\eta| < 3.1$ .

Very important point is a choice of photoelectron device, which converts the Cherenkov light into an electronic pulse. In comparison with PMTs used in such detectors at RHIC and LHC, a multianode MCP-PMT Planacon, recently developed by Photonis [10, 11], has more promising features. The emergence of Planacon provoked wide spread development

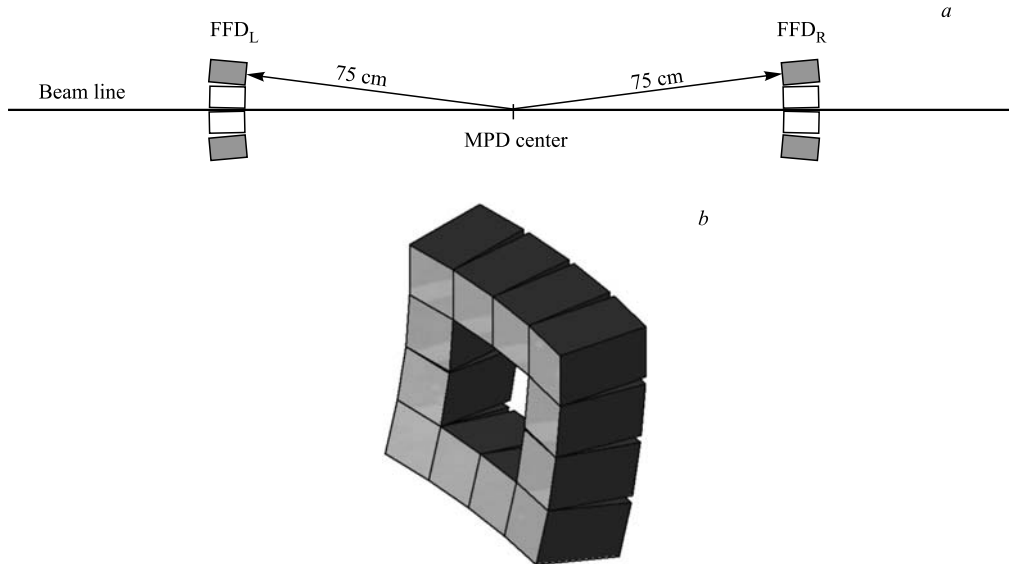


Fig. 1. Layout of the FFD along the beam line (*a*) and schematic view of the FFD subdetector (*b*)



Fig. 2. View of MCP-PMT XP85012

of advanced detectors with a picosecond time resolution for present and future experiments, BaBar [12], ATLAS [13], Belle [14], LHCb [15], and PANDA [16]. This device, shown in Fig. 2, has rectangular form with a photocathode of  $53 \times 53$  mm, which is sensitive in visible and ultraviolet region and occupies 81% of the front surface. This is very important for designing fast Cherenkov detectors with dense packing of a definite number of PMTs into a large-scale detector array.

The MCP-PMT Planacon XP85012/A1, chosen for the FFD counters, has a matrix-like  $8 \times 8$  multianode topology. The inner chevron assembly of two MCPs with  $25\text{-}\mu\text{m}$  channels gives a typical gain factor of  $\sim 10^5\text{--}10^6$ , depending on a value of high voltage applied. Good linearity of output pulses with the 0.6-ns rise time, the transit time spread  $\sigma_{\text{TTS}} \sim 37$  ps [17], and low noise are important characteristics, providing picosecond time resolution of the FFD. High immunity to the magnetic field of the MCP-PMTs is the crucial factor for detectors' operation because the FFD will function in strong magnetic field of the MPD with  $B = 0.5$  T.

Careful experimental tests with picosecond lasers, relativistic beams of single-charged particles, and in magnetic fields with ramping up from zero to 1.5 T were carried out by different groups to study the most critical characteristics of the MCP-PMTs for developing a new generation of detectors with picosecond time resolution [14, 16–18]. These studies showed the following: (i) signals from anode pixels are characterized by fairly flat response with variation factor of 1.5 with rather low cross talk; (ii) the single photon time resolution does not depend on the magnetic field; (iii) Planacon XP85012 has stable operation up to the single photon rate  $\sim 1$  MHz/cm<sup>2</sup> at gain  $10^6$ ; (iv) the lifetime depends on the integrated anode charge, and it was found that for XP85012 the gain decreases only by a factor of 0.9 with increasing anode charge up to 100 mC/cm<sup>2</sup> (in addition, experts of Photonis claim that lifetime of Planacon devices has recently been much increased). The last characteristic leads to the conclusion that the FFD counters based on MCP-PMTs XP85012 will operate without essential change of their characteristics during about 10 years of beam time. This estimation is based on the beam conditions planned for MPD/NICA, results of our simulation, and low gain regime of the MCP-PMT operation.

Following experience of other groups [17] and our test results, operation of Planacon at low gain demonstrates good time resolution and gives some advantages. It has better

aging properties and rate issues. By lowering the gain, the FFD counter becomes sensitive only to relativistic charged particles traveling through the Cherenkov radiator and does not see a background with a few photoelectron deposits from  $\gamma$  rays. Each high-energy photon coming from IP produces several energetic electrons in Pb plate. The electrons pass through the radiator and generate high response of MCP-PMT. Additional amplification by a factor between 30 and 100 is provided by fast front-end electronics (FEE) of the counter.

The radiator has to be thick enough to get rather large number of photoelectrons  $N_{pe}$  from photocathode and a sufficient signal-to-noise ratio for good timing. The radiator bars with polished sides are made of fused quartz. The measurements performed by several groups show that the time resolution degrades very rapidly as  $N_{pe}$  goes down for shorter radiator length, and one needs at least 10-mm-thick radiator plus 2-mm-thick window, or  $N_{pe} \sim 30$  photoelectrons, to get good time resolution  $\sigma_t$  at low gain. The MCP-PMT contribution  $\sigma_{MCP-PMT}$  to  $\sigma_t$  falls down as  $N_{pe}$  or radiator length increases, but the fraction from radiator  $\sigma_{rad}$ , due to spread of arrival time of Cherenkov photons on the photocathode, grows as the radiator length increases. The total sigma has a minimum around the length of 17 mm [17]. Thus, our choice of the quartz radiator length in the FFD counters is 15 mm plus 2-mm-thick window.

The time resolution can be estimated by formula

$$\sigma_t \approx (\sigma_{MCP-PMT}^2 + \sigma_{rad}^2 + \sigma_{PB}^2 + \sigma_{PS}^2 + \sigma_{elec}^2)^{1/2},$$

where  $\sigma_{PB}$  — contribution of anode pixel broadening effect;  $\sigma_{PS}$  — contribution of path spread for pixels joined together into one pad;  $\sigma_{elec}$  — time resolution of electronics. In ideal case for FFD counter, one obtains  $\sigma_t \sim 10$  ps for a single detector channel. Here the following quantities were taken:  $\sigma_{MCP-PMT} = \sigma_{TTS}/\sqrt{N_{pe}} \approx 37 \text{ ps}/6 \approx 6 \text{ ps}$ ,  $\sigma_{PS} = 0$  ps, and  $\sigma_{elec} = 5$  ps. In experiments with detectors based on MCP-PMTs, typical values of  $\sigma_t$  lie between 20 and 30 ps, and only the best results show  $\sigma_t < 15$  ps.

It is important to note that for Au + Au collisions, typically not one but several channels of each of the FFD subarrays will produce the pulses for timing. Using statistical methods over multiple simultaneous measurements, one can essentially reduce the uncertainty of start signal.

The main parts of the detector are schematically shown in Fig. 3, which are two FFD arrays with FEE, subdetector electronics, Vertex/L0-trigger electronics, readout electronics, and ps-laser calibration system.

The FFD subdetector array consists of 12 identical modules (counters) where each module has a  $2 \times 2$  cell structure. So the total number of independent electronic channels is 48. Each module consists of a lead converter, a set of four quartz radiator bars, MCP-PMT XP85012/A1, and fast front-end electronics (FEE) as a source of signals for readout and Vertex/L0-trigger. The MCP-PMT with 64 anode pads is transformed into the 4-channel photodetector by merging 16 pads ( $4 \times 4$ ) of each cell into a single channel. Each FEE channel produces LVDS and analog signals which are fed to FFD electronics.

In addition to the anode pads signals, the Planacon XP85012/A1 has a common MCP output signal. The time resolution obtained with this signal in [14] was slightly worse than the result obtained with anode signal. Our test measurement confirms this conclusion. We plan to use these signals from all the counters of both the FFD subarrays for generating pseudo-Vertex and L0-trigger signals. For this purpose, an additional channel with amplifier and discriminator is added to the FEE board.

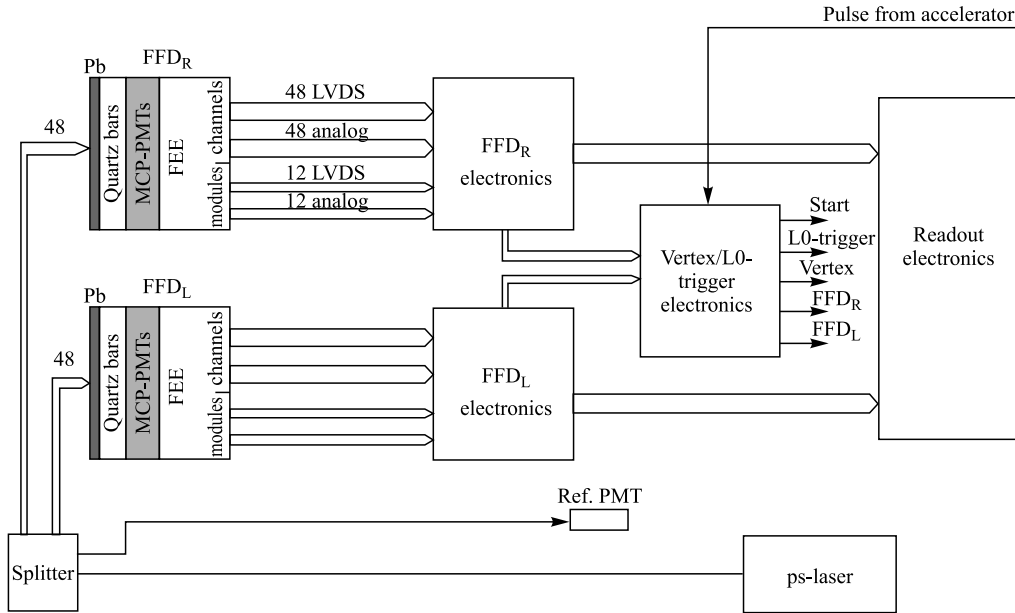


Fig. 3. FFD system

At a moment two approaches for readout electronics are considered: fast digitizing of pulse shape of analog signals and the TDC32VL modules [19], used in the TOF detector. This module is the VME64x 32-channel LVDS 25 ps multihit timestamping TDC developed and produced in the Laboratory of High Energy Physics, JINR.

A ps-laser system will be applied for calibration and monitoring of the FFD during its operation. Here the experience with PiLas diode lasers obtained in other laboratories will be used. The laser beam is split into 96 + 1 channels. The pulses are fed through optical cables to the front surfaces of quartz bars, and the single channel is needed for reference signal.

The aim of the present R&D stage is (i) developing projects and prototypes of these systems and (ii) studying characteristics both in special test measurements and by MC simulation.

## 2. MONTE CARLO SIMULATION

The UrQMD NICA plus GEANT3 code was applied to Monte Carlo (MC) simulation of Au + Au collisions to study trigger and time performance of the FFD. So 1-mm aluminum beam pipe, magnetic field of 0.5 T, lead layer with thickness of 7 mm to convert photons to electrons as well as FFD geometry and materials were taken into account. The  $z$  positions of collision points have a Gaussian distribution around the center of MPD.

First, characteristics of photons and charged particles coming into the FFD were simulated. The energy spectrum of photons in Au + Au collisions at  $\sqrt{s_{NN}} = 5$  GeV is shown in Fig. 4. The spectrum covers a broad energy range and indicates that most photons have to fall within the interval from 100 MeV to a few GeV. The distributions of protons and charged pions, produced in central collisions into the FFD solid angle, are given in Fig. 5 as a function of

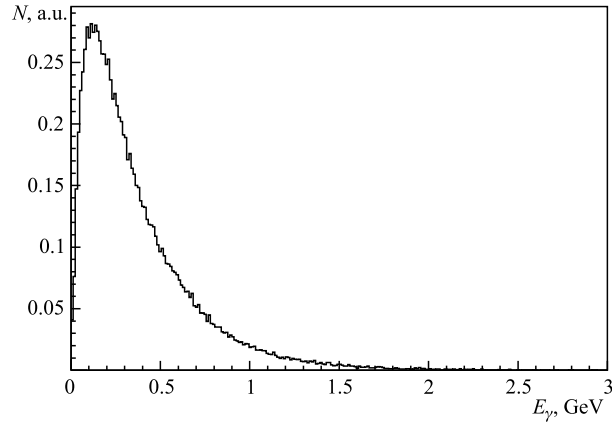


Fig. 4. Energy spectrum of photons passing through the front surface of FFD array for Au + Au collisions at  $\sqrt{s_{NN}} = 5$  GeV

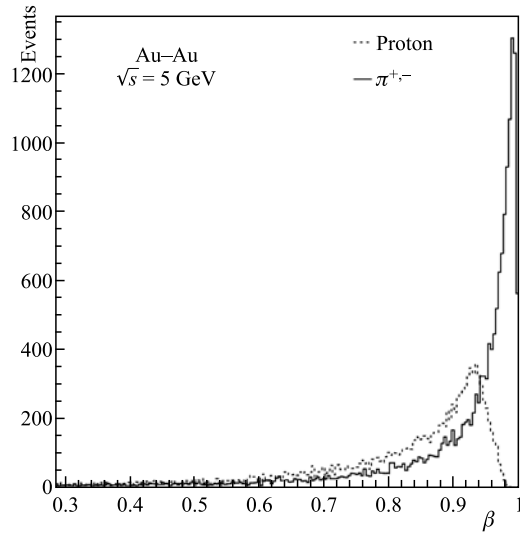


Fig. 5. Distributions of protons and pions arriving at FFD over velocity  $\beta$  for Au + Au central collisions at  $\sqrt{s_{NN}} = 5$  GeV

velocity  $\beta$  for the same energy of colliding nuclei. In quartz, the Cherenkov light can be produced by charged particle with  $\beta$  exceeding threshold value  $\beta_{th} \approx 0.69$ .

The distribution of photon multiplicity as function of an impact parameter is shown in Fig. 6, *a*. For central collisions, some photons with a number varying from 1 to 15 pass through the lead converter of each FFD subdetector. The mean number of these photons falls down with increasing impact parameter. Figure 6, *b* illustrates background of slower charged particles whose velocities exceed the threshold value of Cherenkov radiation in quartz. These particles are evaluated with the multiplicity of 10–30 and the time of flight less than 3.5 ns. The impact of charged particles on the detector characteristics is under investigation. The strong velocity dependence of Cherenkov radiation intensity decreases this

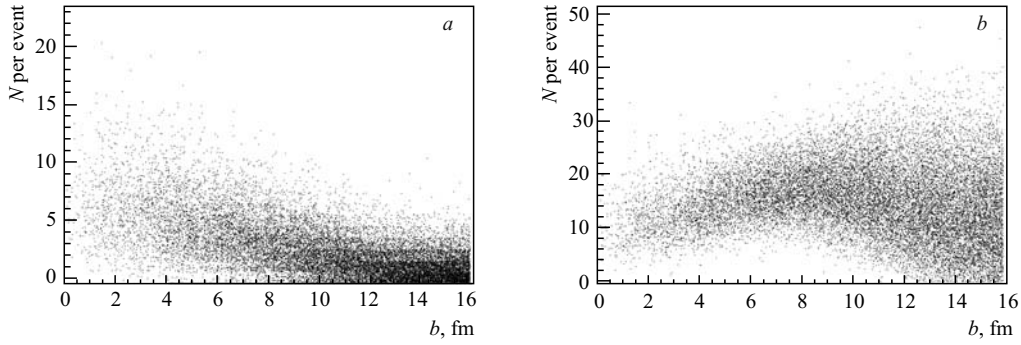


Fig. 6. Photon multiplicity distribution in the acceptance of single FFD subdetector as a function of impact parameter for Au + Au collisions at  $\sqrt{s_{NN}} = 5$  GeV (a), and the same for charged particles with velocities above threshold value of the Cherenkov radiation in quartz (b)

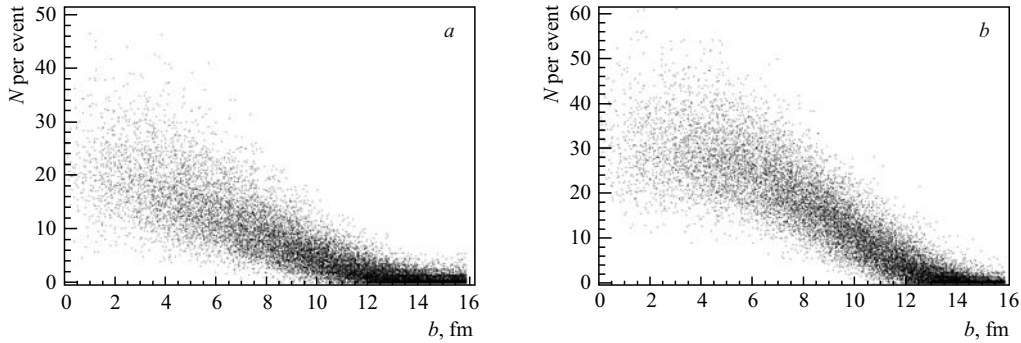


Fig. 7. The same as in Fig.6 but for Au + Au collisions at  $\sqrt{s_{NN}} = 9$  GeV

effect. It is important to stress that only pions and protons with momenta higher than 132 and 885 MeV/c, respectively, produce the Cherenkov light in quartz, giving contribution to the FFD response.

Similar distributions for Au + Au collisions at  $\sqrt{s_{NN}} = 9$  GeV are shown in Fig. 7. Here, the mean photon multiplicity in central collisions essentially exceeds the value found in the first case of lower energy. The numbers of photons and charged particles coming into the detector acceptance strongly depend on centrality decreasing with the impact parameter. Mean multiplicities of photons and charged particles grow as beam energy increases; therefore, the observed correlation between the FFD response and the impact parameter becomes clearer.

Thus, MC simulation helps reveal that the mean number of photons and charged particles depends on centrality of the collisions at the highest energies. To separate central, semicentral, and peripheral collisions, the FFD information, such as a sum amplitude of output signals and/or these signals number, can be used in combination with data from other fast MPD detectors, like Zero Degree Calorimeter.

Induced by a primary high-energy photon in the lead converter, electrons of  $\beta \approx 1$  generate a number of Cherenkov photons in the quartz radiator, and approximately 20% of these photons produce photoelectrons outcoming from a photocathode of the MCP-PMT. The MC simulation estimates the mean multiplicity of the photoelectrons to be over 30 pe for

the 15-mm quartz radiator attached to the 2-mm window of the MCP-PMT and, as discussed earlier, it is a necessary condition for good time resolution of the detector.

Additionally, a background of low energy electrons traveling in magnetic field along the beam line was studied by means of MC simulation. These electrons hit the radiators of FFD modules and produce small responses, which are randomly distributed over time scale. We found that the intensity of these background events is rather low and slightly influences detector response and its time characteristics.

The estimated efficiency of registering Au + Au collisions with a single FFD array at four different energies  $\sqrt{s_{NN}} = 5, 7, 9,$  and 11 GeV and 30-pe bias is shown in Fig. 8.

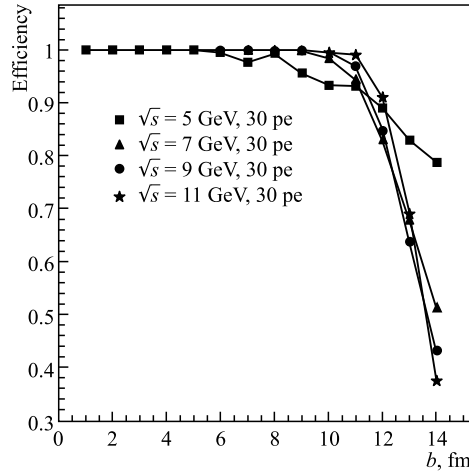


Fig. 8. Efficiency of FFD subdetector with bias of 30 pe as a function of impact parameter for registering Au + Au collisions at four different energies  $\sqrt{s_{NN}} = 5, 7, 9,$  and 11 GeV

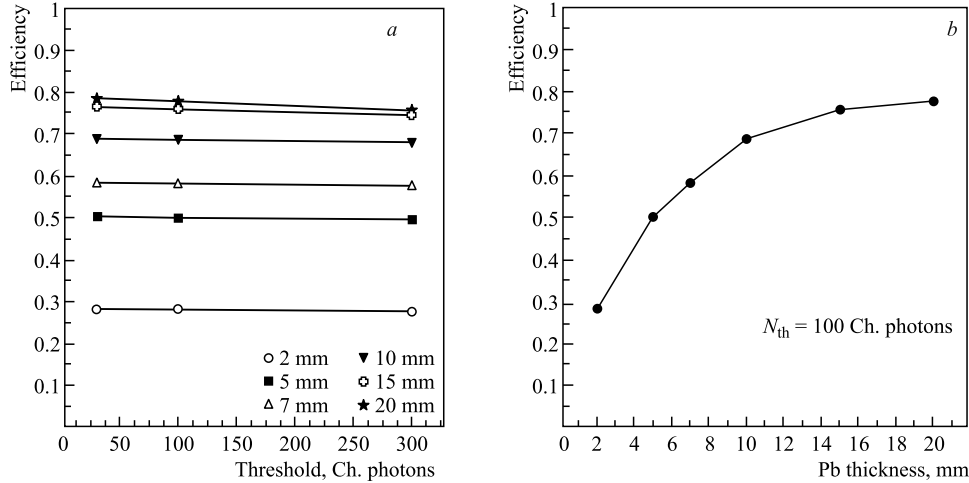


Fig. 9. Efficiency of single photon registration: a) vs. bias on multiplicity of the Cherenkov photons at different thickness of the lead converter, b) vs. thickness at the fixed bias of 100 Cherenkov photons

For collisions at 5 GeV, the efficiency is  $\sim 1$  at impact parameters  $b < 6$  fm; then it falls down to 0.9 when  $b$  grows up to 12 fm. At higher energies, the efficiency is  $\varepsilon \approx 1$  for  $b < 10$  fm.

It is known that efficiency of photon registration depends on thickness of the lead converter. The results of simulation of single photon registration by FFD array is shown in Fig. 9 for energy spectrum of the photons given in Fig. 4. The lead thickness was selected by steps of a few mm within an interval from 2 to 20 mm. The efficiency grows with lead layer increasing; however, this interrelation becomes weak if thickness exceeds 10 mm. For a final FFD design, the thickness of lead layer should be presumably increased up to the value of 10 mm, which could raise the efficiency by a factor of  $\sim 1.19$ . It is important for operation of the detector at energies  $\sqrt{s_{NN}} < 5$  GeV, where the photon multiplicity is low.

### 3. PROTOTYPE OF FFD MODULE

As was noted earlier, FFD subdetector array consists of 12 modules. The prototype modules have dimensions of  $6.1 \times 6.1 \times 10$  cm. The fused quartz radiators are attached to window of MCP-PMT through special optical grease with high transparency for UV photons. The FEE board sits directly on the XP85012/A1 connectors. Each quartz bar has the transverse dimensions of  $26.5 \times 26.5$  mm and is 15 mm thick, and its side surfaces are covered with aluminized mylar to reflect the Cherenkov photons to the photocathode. The total radiator transverse dimensions of  $53 \times 53$  mm are equal to an active area of the photocathode.

The internal content of the module is schematically shown in Fig. 10, *a*. A view of two prototypes and their components (quartz radiators, MCP-PMTs, FEE board, and module housing with signal, HV and LV connectors) are shown in Fig. 10, *b*.

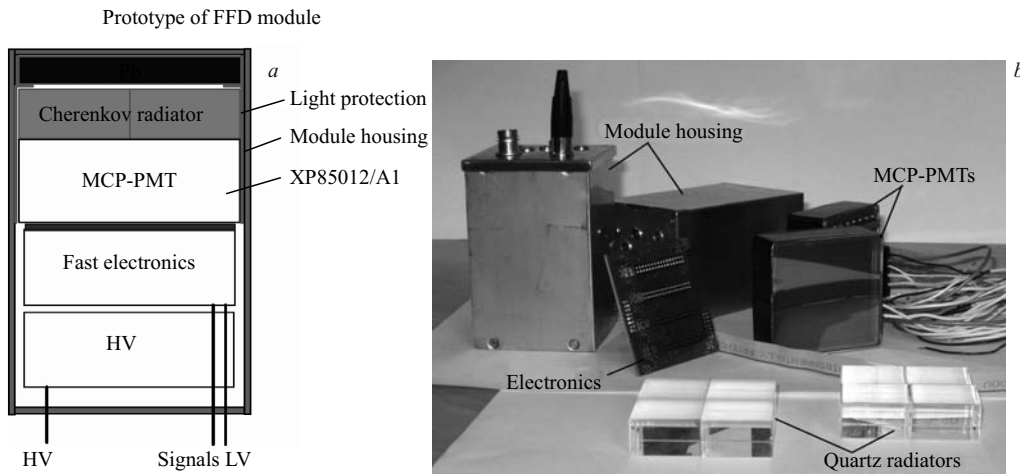


Fig. 10. A module scheme (*a*) and a view of module prototypes with their components (*b*)

#### 4. MODULE ELECTRONICS

Functional scheme of each FEE channel is given in Fig. 11. Major elements are a low-noise input amplifier with BFR93A transistor, a pulse shaper minimizing signal-to-noise ratio, an RC chain filtering signal frequency, a fast amplifier of  $\sim 40$  dB gain with MAR-8 chip of DC — 8 GHz bandwidth, and LMH6703 discriminator (1.2 GHz, Low Distortion Operational Amp). Analog output pulses with  $\sim 2$ -ns rise time are transmitted to readout electronics through a coaxial cable, while the discriminator provides logic signals of the LVDS standard.

The FEE board is shown in Fig. 12. The board bears on five identical channels, where four channels accept signals from the anode pads, as shown in Fig. 11. One more channel accepts and handles a signal from the specific MCPs output.

The length of LVDS pulses depends on a pulse height of MCP-PMT signal. The pulses with the maximal width correspond to signals with the largest amplitudes induced by high

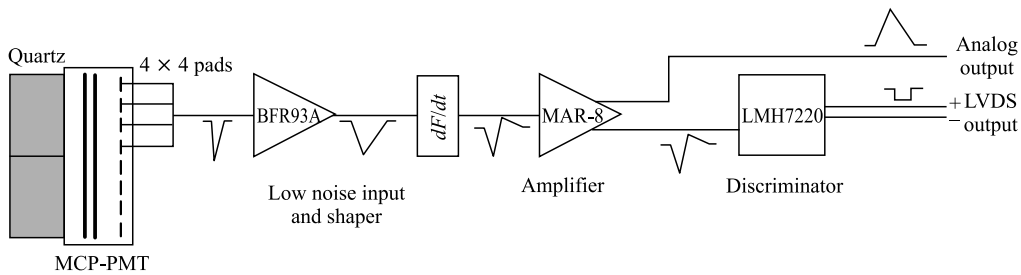


Fig. 11. Functional scheme of the FEE channel

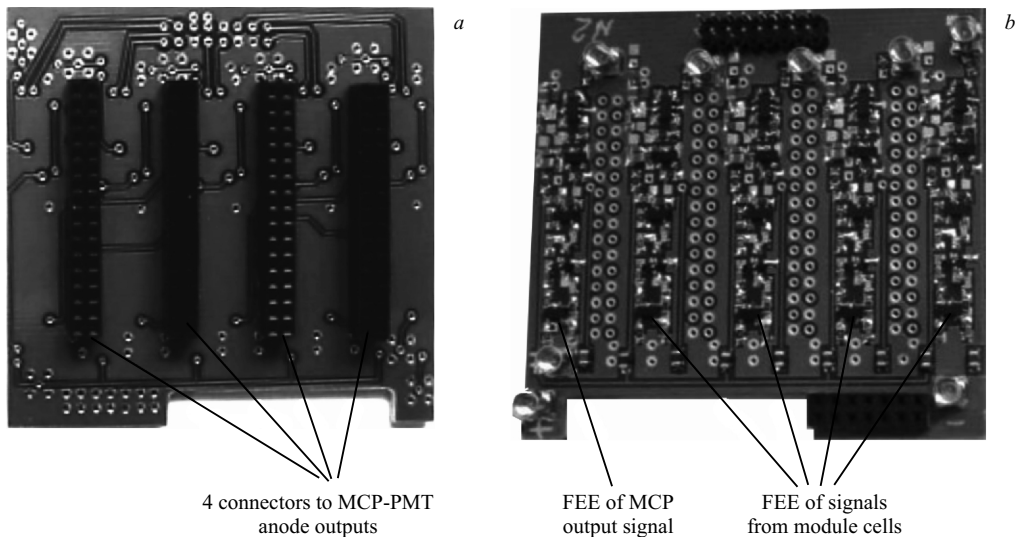


Fig. 12. A view of the FEE board: *a*) front side with connectors to the MCP-PMT; *b*) back side with mounted electronics

energy photons. One may expect that arrival of several particles in one quartz bar can change timing characteristics of output signal. To study this effect, new MC simulation will be fulfilled in the future.

## 5. EXPERIMENTAL TESTS

Some preliminary tests with the 1-ns light pulses from an LED source demonstrated a necessity of careful design of the FEE inputs, which should provide a minimum time dispersion of signals accepting from individual anode pads. In particular, a time jitter of  $\sim 15\text{--}20$  ps was estimated for the present FEE design. For further improvement of timing, a new version of FEE board is developed.

The first results on response and time resolution of the FFD module were obtained in test measurements with proton beam of JINR Nuclotron and cosmic muons.

Block diagram of readout electronics used in the test measurements is shown in Fig. 13.

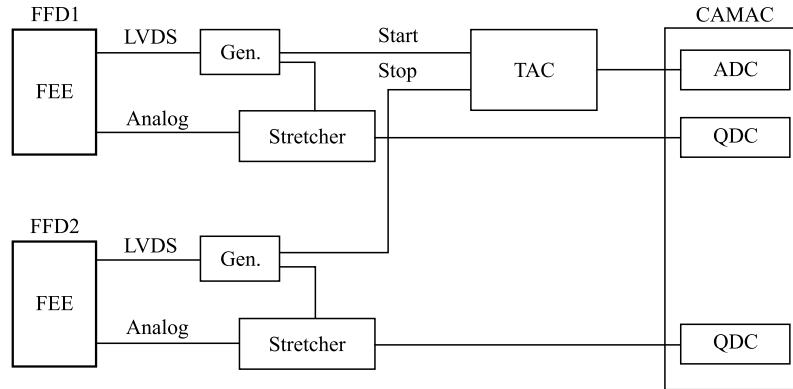


Fig. 13. Block diagram of readout electronics used in the test measurements

The electronics was developed in the Radium Institute, St. Petersburg. It is based on a specialized module which provides pulse transformation and processing. Main module parts are event selection logic, time-to-amplitude converter (TAC), and pulse amplitude stretcher with charge amplifier [20]. Output signals are directed to analog-to-digital converters of the 4ADC-331 type from JINR, charge-to-digital converters of the 8QDC-16136 type also from JINR, and input register (not shown in Fig. 13). Time-of-flight measurements are performed with the 32-ps time bin.

In the measurement with proton beam of the 1.95-GeV energy, the protons were randomly distributed within  $\sim 2$ -s bunch of the  $\sim 300$  protons/bunch intensity. A typical distribution of pulse height measured with the LeCroy oscilloscope (panel *a*) and ADC (panel *b*) is shown in Fig. 14.

The pulses induced by protons have a rather low dispersion of amplitudes, besides a large empty gap between these pulses and noise. The latter observation is confirmed by a distinct

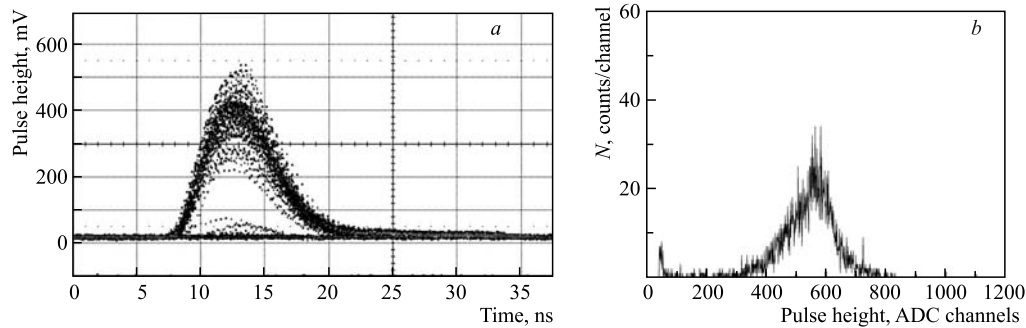


Fig. 14. Typical distribution of pulse height measured with the LeCroy oscilloscope (a) and ADC (b) for protons of the 1.95-GeV energy

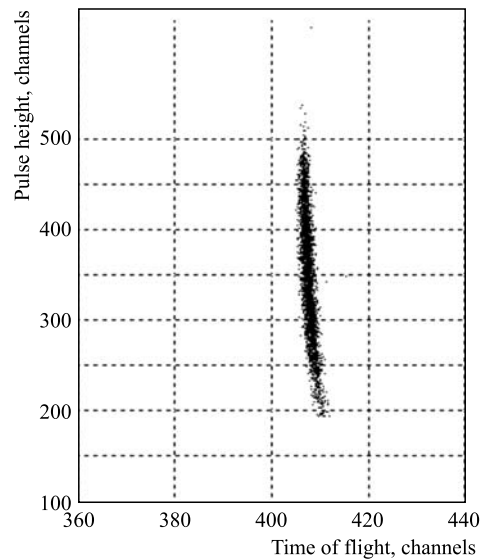


Fig. 15. Typical  $t$ - $A$  plot obtained in measurements with the 1.95-GeV protons

proton peak on the ADC scale. Thus, these distributions indicate a rather high number of photoelectrons needed for a good time resolution.

A typical time–amplitude distribution of events for single channel of the detector ( $t$ - $A$  plot) is given in Fig. 15. This distribution is necessary to find a correction function for experimental data processing. Such corrections are made for both modules, leading to essential decrease in the TOF peak width.

The TOF distributions obtained for the 1.95-GeV protons with and without  $t$ - $A$  correction (slewing effect) are presented in Fig. 16. As a result of the correction, the Gaussian shape indicates  $\sigma \approx 42$  ps, which corresponds to  $\sigma_t \approx 30$  ps for a single channel of the detector.

Tests with cosmic muons were fulfilled in the Radium Institute, St. Petersburg. The experimental setup consisted of a counter with thin plastic scintillator, two tested FFD modules

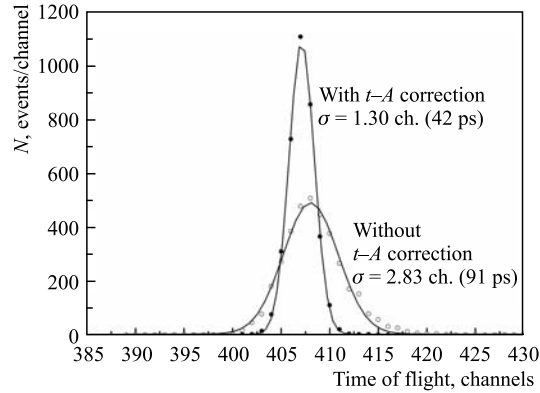


Fig. 16. TOF distributions for the 1.95-GeV protons with and without  $t-A$  correction

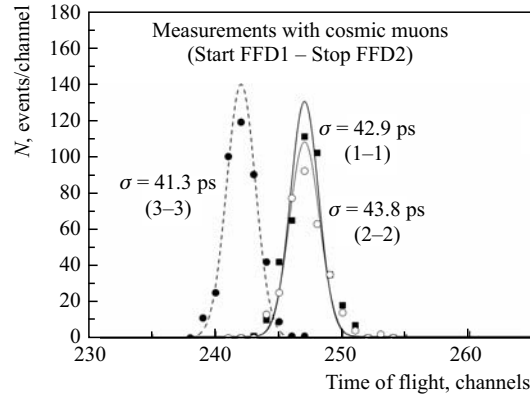


Fig. 17. TOF distributions obtained in the measurements with cosmic rays

with the flight distance of 15 cm between them, and a detector with 10-cm-diameter styrene crystal placed behind 20-cm lead absorber. The duration of typical run was about one week, and  $\sim 3000$  cosmic events were taken within this period. The TOF spectra with  $t-A$  correction for three combinations of the FFD1–FFD2 channels (1–1, 2–2, and 3–3) are shown in Fig. 17. The TOF peaks have  $\sigma \approx 41\text{--}44$  ps, which corresponds to  $\sigma_t \approx 29\text{--}31$  ps for single channel of the detector.

Finally, we can declare that the time resolution of  $\approx 30$  ps has been obtained from experimental tests with present FFD prototypes with proton beam and cosmic rays. Taking into account the mentioned time jitter of FEE, we expect even better results after upgrading FEE in the future.

## CONCLUSIONS

The concept of Cherenkov FFD is registering high-energy photons from prompt decays of neutral pions. Its aim is to provide fast and effective triggering of Au + Au collisions at the center of the MPD/NICA setup at rather low energies, several GeV per nucleon, and to

generate precise start signal with  $\sigma_t < 50$  ps for the TOF detector. Application of advanced photodetectors, based on Planacon MCP-PMTs from Photonis, in the FFD modules allows for design of compact multichannel detector array with high time characteristics, low sensitivity to charged particle background, and good operation in MPD magnetic field during not less than ten years of beam time.

The MC simulation of the FFD performance shows that the efficiency of registering central and semicentral Au + Au collisions in energy range  $\sqrt{s_{NN}} \geq 5$  GeV by single FFD array with 7-mm lead converter is close to 100%. In the future, we plan to apply 10-mm lead plates in the FFD modules to increase the efficiency of photon detection and, by means of this, raise the efficiency of collision triggering at lower beam energies.

The two prototypes of FFD module were designed, manufactured, and tested with LED, proton beam and cosmic rays. The obtained time resolution for single detector channel is  $\sigma_t \approx 30$  ps, and it is about twice as good as the required value. The measured detector responses for single charged particles with  $\beta \approx 1$  correspond to 20–30 pe.

Further improvement of FFD module characteristics is planned. The number of photoelectrons will be increased by applying new photodetectors MCP-PMT XP85012/A1-Q with quartz window and quantum efficiency of 18% at wavelength of 200 nm. A new version of FEE board is also under development to improve time characteristics.

The R&D stage will take next two years till the end of 2014. It includes development and study of the detector subsystems, such as prototypes of the detector module and the front-end electronics, the logic and electronics of Vertex/L0-trigger, the readout electronics, and the ps-laser calibration system. For experimental tests, some special stands will be constructed and new measurements with beams and cosmic rays will be carried out. At this period, we also plan to continue studying the detector performance by means of MC simulation. First of all, the simulation of time responses of FFD modules for events with different particle multiplicity will be investigated. Another important issue for the simulation is more careful study of background particle contribution to the detector responses.

**Acknowledgements.** The authors are grateful to V.M. Golovatyuk, N.M. Piskunov, and P.A. Rukoyatkin for their co-operation and kind assistance during test measurements with proton beams. The authors also thank experts of Photonis E. Schyns and J. DeFazio for fruitful discussion of Planacon application in our measurements.

#### REFERENCES

1. *Sissakian A., Sorin A.* // CERN Courier. 2010. V. 50(1). P. 13; <http://mica.jinr.ru>.
2. *Abraamyan Kh. U. et al.* // Nucl. Instr. Meth. A. 2011. V. 628. P. 99.
3. *Ikematsu K. et al.* // Nucl. Instr. Meth. A. 1998. V. 411. P. 238.
4. *Allen M. et al.* // Nucl. Instr. Meth. A. 2003. V. 499. P. 549.
5. *Back B. B. et al.* // Ibid. P. 603.
6. *Bengtson B., Moszynski M.* // Nucl. Instr. Meth. 1970. V. 81. P. 109.
7. *Bondila M. et al.* // IEEE Trans. Nucl. Sci. 2005. V. 52. P. 1705.
8. *ALICE Collab.* The T0 Detector. ALICE TDR 011, CERN-LHCC-2004-025. 2004.
9. *Zhou J.* Construction of a New Detector and Calibration Strategies for Start Timing in the STAR Experiment at RHIC. Master's Thesis. Rice Univ. Houston, Texas, 2006.
10. [www.photonis.com](http://www.photonis.com)

11. *Schyns E.* // Workshop on Large Area Photo-Detectors, Electronics for Particle Physics and Medical Imaging, Clermont Ferrand, Jan. 28, 2010.
12. *Va'vra J. et al.* Report SLAC-PUB-12803. 2007.
13. *Albrow M. G. et al.* Quartz Cherenkov Counters for Fast Timing: QUARTIC. arXiv:1207.7248v1 [physics.ins-det]. 2012.
14. *Korpar S. et al.* // Nucl. Instr. Meth. A. 2009. V. 595. P. 169.
15. *Garcia L. C.* // DT Detectors Physics Meeting. CERN, 2011.
16. *Lehmann A.* // RICH 2010, Cassis, France, May 2010.
17. *Va'vra J. et al.* // Ibid. Report SLAC-PUB-14279. 2010.
18. *Britting A. et al.* // Workshop on Fast Cherenkov Detectors, Giessen, April. 2011. 2011 JINST 6 C10001.
19. Internet site: [afi.jinr.ru/TDC32VL](http://afi.jinr.ru/TDC32VL)
20. *Batenkov O.I. et al.* // Nucl. Instr. Meth. A. 1997. V. 394. P. 235.

Received on September 19, 2012.